Contents lists available at ScienceDirect

Polymer Testing

Quantification of sulfur distribution on rubber surfaces by means of μ-X-ray fluorescence analysis

S. Frosch [a], V. Herrmann [a], F. Grunert [b],[*], A. Blume [b]

[a] Technical University of Applied Sciences Würzburg-Schweinfurt, Germany
[b] University of Twente, Faculty of Engineering Technology, Department of Mechanics of Solids, Surfaces & Systems (MS3), Chair of Elastomer Technology & Engineering, Enschede, the Netherlands

ARTICLE INFO

ABSTRACT

A homogeneous distribution of sulfur in a rubber compound is often desired. Spatially resolved imaging techniques are useful for evaluating the distribution of this crosslinking chemical. Typical measurement methods such as SEM (scanning electron microscopy) or TEM (transmission electron microscopy) have very high resolutions. However, the sample size or the maximum area to be investigated is limited, which makes it difficult to obtain a statistically reliable determination of sulfur homogeneity across the component or sample.

In this work, an alternative measurement technique is therefore presented: the μ-XRF (μ-X-ray fluorescence analysis). With the help of this method, it is possible to scan surfaces of several cm^2 and to show the distribution of different chemical elements. Its measuring principle has been known for decades but has hardly been used in the rubber industry so far.

The main reason for this is that its quantification process for polymeric samples is more complex than for geologic or metallic samples, which are typically been investigated with μ-XRF to date. In this paper, this issue is addressed and a solution is presented: With the help of the fundamental parameter method, the determination of sulfur homogeneity and distribution on rubber surfaces becomes possible. This opens up a variety of further possibilities for the use of μ-XRF in the rubber industry: For example, it could be used in areas of tire production, recycling of end-of-life rubber, and beyond.

1. Introduction

Sulfur is an essential component of rubber compounds as it forms crosslinks that give the material its characteristic elastic behavior. Typically, a homogeneous distribution of sulfur is targeted in order to obtain a homogeneous distribution of network points [1–3]. This enables properties that are as uniform as possible throughout the overall compound.

Typical analytical methods evaluating elemental distributions on sample surfaces are SEM with energy dispersive X-ray detection (EDX), TEM with EDX or X-ray photoelectron spectroscopy (XPS) [4]. All examination methods have in common that surfaces up to a few mm^2 can be examined very precisely with resolutions (spot distances) in the nanometer to micrometer range. This resolution is demanded for answering various scientific questions. However, this resolution is not suitable for evaluating the sulfur homogeneity of a rubber sample. This is because a significantly larger sample surface area would have to be measured in order to generate statistically relevant data.

A measurement method that is suitable for this purpose is the μ-X-ray fluorescence analysis (μ-XRF): Similar to SEM, the sample is scanned with an excitation beam. However, it uses an X-ray beam and not one consisting of electrons. Its diameter is approx. 25 μm and thus 1.000 times larger than that of the SEM [5]. This lowers the resolution limit of the method, so that general dispersion investigations cannot be examined with this method. However, it makes it possible to screen significantly larger areas to reveal distributions of different rubber compound components. In the device chosen for this work, areas of several cm^2 are feasible to be examined. The X-ray beam is able to excite electrons in the sample. The resulting fluorescence radiation and therefore chemical elements distributions can be displayed.

The μ-XRF is thus able to analyze large and therefore statistically reliable areas for sulfur distribution. Furthermore, the method is particularly suitable for the evaluation of blends [6] and tires [7], for example. The latter consist of several different layers, which can be

* Corresponding author.
  E-mail address: f.grunert@utwente.nl (F. Grunert).

visualized exceptionally well with μ-XRF, see Fig. 1. Furthermore, the method can be used to investigate sulfur migration in samples containing ground rubber (GR) from end-of-life rubber [8–11]. GR is (cryo-) mechanical cut and shredded vulcanized end of life rubber with grain sizes between 0.08 and 2 mm [11,12]. Thus, the μ-XRF is a method that gives useful information from rubber manufacturing to recycling.

Quantification of the results subsequent to the analysis is necessary in order to obtain information about real concentration differences. These can then be expressed, for example, in the unit parts per hundred rubber (phr). To date the μ-XRF has hardly been used for the investigation of rubber material, some examples are given in Refs. [13–17]. This can be attributed to the fact that quantification, in particular, can become a very complex step subsequent to measurement [18,19]. At the same time, numerical quantification of elemental distributions is essential for proper evaluation of the measurement results. Thus, the purpose of this paper is to provide guidance on how to use μ-XRF to quantify exact concentrations of individual elements on the rubber surface.

Two measurement series of natural rubber (NR) and styrene butadiene rubber (SBR) form the basis of the sulfur quantification. These carbon black-filled specimens are prepared as a reference for the sulfur signal detected by μ-XRF. Furthermore, the sulfur content of these samples was determined using the independent method "832 Series Sulfur/Carbon Determinator" by LECO Corporation [20] to verify the findings from μ-XRF. This analytical method has successfully been used in previous studies to validate the quantification of sulfur via XRF [21].

2. Experimental setup

2.1. Compound formulations and mixing conditions

For each type of rubber (NR, SBR) a separate reference series with different sulfur contents was produced. The concentrations for sulfur and accelerator (CBS) - because the latter also contains sulfur and to keep the ratio of sulfur and accelerator constant - are increased within these series from 0.4 to 3.0 phr, see Table 1. Both reference series thus consists of six samples.

Table 2 gives a more detailed overview about the compound components:

First, the NR was masticated in an internal mixer (Werner & Pfleiderer, 1.5 l, PES3). For each sample, 1 kg of NR was masticated for 20 min at 20 rpm and a temperature of the mixer of 25 °C [22].

The base compounds were produced in the same internal mixer at 40 rpm, 50 °C and an effective volume V_{eff} of 70% in the following mixing procedure [22,23]:

- 0': Polymer
- 1': ZnO, St. Acid, Carbon Black
- 2,30': Cleaning step
- 4,30': Dump

After controlling the weight of each sample, the compounds were cooled down on the laboratory mill (Schwabenthan 200 × 450; both rollers 20 rpm, gap: 2.5 mm, 40 °C) for 1 min.

Then, the final compounds (identical conditions as for base compounds) were mixed in the following mixing procedure:

- 0': Base compound, CBS, sulfur
- 3': Dump

After dumping and weighing of the compound, it was cooled down again on the laboratory mill (front roller 16 rpm, back roller 20 rpm, gap: 2 mm at 40 °C):

- 0': Final compound on laboratory mill
- 1': Cutting three times left and right, rolling up at a gap of 1 mm
- 4': Gap: 2.5 mm, both rollers at 20 rpm; dump

2.2. Vulcanization behavior

A SIS V50 from TA Instruments (former Scarabaeus) was used to determine the vulcanization curves of all samples at 160 °C. Each compound was tested three times. A heating press (Collin Plattenpresse 200) was used to vulcanize the specimens to t95. Samples with thickness of 2 mm were produced for 832 Series Sulfur/Carbon Determinator. Specimens of 6 mm thickness were vulcanized to be measured by μ-XRF. Due to the increased thickness, those samples were vulcanized to t95 + 2 min. The specimens examined by μ-XRF have the following dimensions: 10 × 10 × 6 mm (length x width x height). They were taken centrally from larger rubber sheets (130 × 117 × 6 mm).

2.3. Micro X-Ray fluorescence analysis

In 1895, Wilhelm Conrad Roentgen discovered the X-rays in Wuerzburg, Germany [24]. Since then, many different analytical methods were invented using X-rays for the investigation of both, humans and materials. Since the 1960s, the X-ray fluorescence analysis (XRF) is a standard examination method e.g. in the metal industry, where it is used for qualification and quantification of individual chemical elements in metallic samples. It is a non-destructive method characterized by its robustness combined with high precision over a wide concentration range [18].

In recent years, this measurement method has been developed further to the imaging μ-XRF [25]. The prefix "micro" indicates the resolution of this method. Today, samples of several cm^2 in size can be examined with spot distances of few micrometers (typically 25 μm).

A Bruker M4 Tornado from company Bruker Nano GmbH was used to analyze the samples of both calibration series. Its X-ray tube – equipped with a target of Rhodium (no filter) – was set to 50 kV and 200 mA and two silicon drift detectors measured the fluorescence radiation. During analysis, the sample chamber was evacuated to 20 mbar absolute to remove the argon present in the ambient air and thus to increase the sulfur signal, since the fluorescence energies of the two elements are very similar. The resolution (distance from one spot to the other) of the measurement was set to 25 μm. Every spot was exposed to radiation for 3 × 40 ms = 120 ms. The selected energy dispersive μ-XRF can detect elements between atomic numbers 11–92 (Na - U). The software Esprit M4 (Version: 1.6.0.286) was used for all measurements and postprocessing.

Fig. 2 shows the working principle of the XRF-technique: Generated X-rays hit the sample surface and eject an electron from the electron shell (left side of Fig. 2). The created vacancy is not stable and is filled by an electron from an outer shell (right side of Fig. 2). The energy released
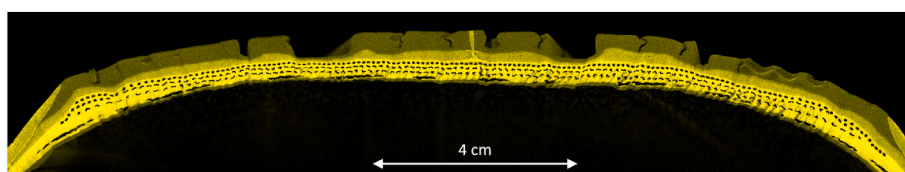

Fig. 1. Qualitative analysis by μ-XRF of an end-of-life passenger car tire: Different shades of yellow indicate different concentrations of sulfur in the plies of the tire. (For interpretation of the references to color in this figure legend, the reader is referred to the Web version of this article.)

Table 1
Compound formulations of the 12 samples in phr.

	Reference series NR						Reference series SBR					
	NR 0.4	NR 0.8	NR 1.2	NR 1.6	NR 2.0	NR 3.0	SBR 0.4	SBR 0.8	SBR 1.2	SBR 1.6	SBR 2.0	SBR 3.0
NR	100						–					
SBR	–						100					
CB	50						50					
ZnO	5						5					
St. Acid	3						3					
Sulfur	0.4	0.8	1.2	1.6	2.0	3.0	0.4	0.8	1.2	1.6	2.0	3.0
Acc.	0.4	0.8	1.2	1.6	2.0	3.0	0.4	0.8	1.2	1.6	2.0	3.0

Table 2
Detailed information about the compound components.

	Name	Company
NR	SIR 20	Weber & Schaer GmbH & Co. KG
E-SBR	Buna SE 1502 L	Arlanxeo Deutschland GmbH
Carbon Black	Corax N330	Orion Engineered Carbons S.A.
ZnO	Zinkoxid Rotsiegel	Brüggemann KG
St. Acid	Edenor ST1 GS	Evonik Industries AG
Sulfur	K46859483 542	Merck Chemicals GmbH
Accelerator CBS	Vulkacit CZ/EG-C	Lanxess Deutschland GmbH

in this process is emitted in form of fluorescence radiation. The amount of fluorescence radiation is characteristic for every chemical element. By measuring this energy, the XRF can determine the excited element. With the μ-XRF, large areas can be screened using this measurement principle. This leads to a mapping ("qualification") of chemical elements.

The energy-dispersive functionality of the used instrument creates a relatively coarse spectrum of results from which the chemical elements can be determined [27]. As a result, only K-transitions of sulfur fluorescence can be measured and thus bonding states of atoms cannot be identified. In comparison, the wavelength dispersive design can do so, because it outputs a finer resolved spectrum [28]. However, this requires a generally much longer measurement time, which makes this mode of operation not feasible for imaging elemental analyses on a larger scale.

Quantification typically is made subsequent to the actual analysis in the postprocessing. There are two different approaches to evaluate measurement results quantitatively: The first method is to work with known compositions using them for calibration of reference samples. Typically, these contain characteristic concentrations of the elements to be determined. By defining the calibration line, a linear relationship between signal intensity and element concentration is thus established.

However, this type of calibration has some disadvantages: For example, the accuracy depends strongly on the homogeneity of the samples. Furthermore, it is only valid for this selected reference material as well as the chosen excitation conditions (tube current and voltage, measurement time, etc.). Even small differences in the sample composition or in the measurement conditions can have the effect of severely limiting the accuracy of the calibration [29].

In contrast, a non-standard-based method would be useful which is independent of sample homogeneity as well as excitation conditions (within the limitations that the conditions are able to excite the respective element). Furthermore, it should work over a large concentration range.

The pioneer of this method is Sherman, who was the first to describe the relationship between signal intensity and concentration mathematically explicitly in 1955 [30]. For the first time, it was possible to use physically defined fundamental parameters (e.g. transition probability, jump ratio, fluorescence yield, linear mass absorption coefficient, etc.) to determine the intensities of individual elements. Since then, further research has been carried out to define these fundamental parameters in a physically explicit way in order to improve the quality of this fundamental parameter method [31]. This standardless quantification method by fundamental parameters shows good results e.g. in geology, as Flude et. all. show [32]. One reason for this is, that the geological samples consist to a significant extent of many chemical elements that are detectable by μ-XRF. Thus, the detected elements represent a sufficiently high fraction of the chemical composition to successfully apply the fundamental parameters.

In contrast, the situation is different for polymer samples: they consist to a large extent of elements that cannot be detected via the used μ-XRF. This includes for example hydrogen, carbon, nitrogen and oxygen (atomic numbers 1, 6, 7 and 8). As column 3 of Table 3 shows, sample SBR 1.2 consists of 62 w% SBR (only C and H in the molecular formula) and 31 w% carbon black (only C). These two components account for approx. 93 w% of the sample substance, which is not detectable via μ-XRF.
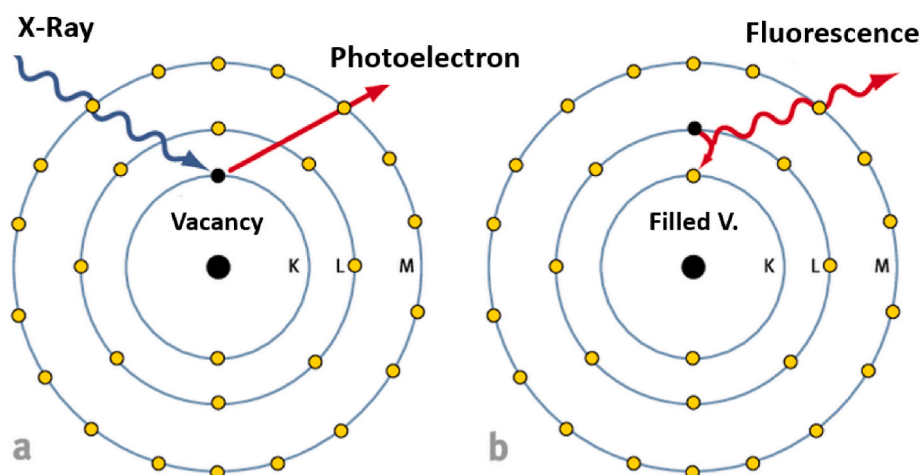

Fig. 2. Generation of fluorescence radiation, adapted from [26].

Table 3
Determination of the sample components of SBR 1.2

	phr	w %	m [g]	Molecular Formula for calculation	M_i [g/mol]	n_i [mol]	n_i [%]
SBR	100	62.3	780.7	$C_{4.9}H_{6.5}$	65.4	11.84	26.3
NR	0	–	–	C_5H_8	–	–	–
Carbon Black	50	31.2	390.3	C	12.0	32.24	71.7
ZnO	5	3.1	39.0	ZnO	81.4	0.48	1.1
St. Acid	3	1.9	23.4	$C_{18}H_{36}O_2$	284.5	0.08	0.2
Sulfur	1.2	0.7	9.4	S	32.1	0.29	0.6
Accelerator	1.2	0.7	9.4	$C_{13}H_{16}N_2S_2$	264.4	0.04	0.1

This "invisible" matter makes the quantification more difficult. The reason for this is that the fundamental parameters can only be applied to detectable elements. This means that only the small fraction of measurable elements - in the example these would be sulfur and zinc - would be qualified by μ-XRF and thus quantified with the fundamental parameter method. Consequently, the polymeric portion would be completely ignored - there would be no concentrations for C and H in the results.

Thus, the fundamental parameter method cannot be used without restrictions for polymer samples. To overcome this, correction elements have to be used. The use of these correction elements can significantly improve the accuracy of this quantification method [29]. For this reason - in addition to the fundamental parameters - the molecular formula of the non-detectable "invisible" material is included in the calculation as the correction element. It is not the chemical sum formula of a real existing compound, but a mathematically calculated one. The way to determine this formula is explained in chapter 3.3.

2.4. 832 Series Sulfur/Carbon Determinator by LECO

The 832 Series Sulfur/Carbon Determinator by LECO Corporation is the alternative method evaluating the sulfur content of the rubber samples. The measurements are performed according to ASTM D 6741 (method B) from 2010. The principle of this analytical method can be described as follows: About 1 g of rubber sample material – cut from plates with thickness of 2 mm – is placed via a combustion boat into a furnace that is set to 1.350 °C and flushed with pure O_2. The sample combusts and the sulfur reacts with the O_2 to SO_2. This gas is then passed on to detection cells for examination. Infrared cells determine the absorption of the wavelengths characteristic for SO_2, allowing the sulfur content of the sample to be specified. It is thus a bulk analysis revealing one sulfur concentration of the entire sample – in contrast to imaging sulfur concentrations with the μ-XRF [20]. It will be termed "LECO" in the following chapters.

LECO is used to determine the sulfur content of a comparatively large sample which can be seen statistically representative for the full compound. In contract, a measurement with SEM-EDX can only quantify a very small sample section and is therefore not necessarily representative for the full specimen. To achieve a fair comparison several individual SEM-EDX measurements could be examined at separated locations of a larger sample. However, this would require a very high amount of time and measurement effort. Furthermore, as mentioned before, this method was chosen because it has already been successfully used as a comparative measurement to XRF [21].

3. Results and discussion

3.1. Vulcanization behavior

Figs. 3 and 4 show the rheometer curves of both reference series. Both depict a similar tendency:
With increasing content of curatives, the torque reaches a maximum

of appr. 37 dNm for NR and SBR. Due to the higher amount of curatives, more crosslinks can be formed that increase the maximum torque of the samples. In contrast to NR, not all SBR-samples show a clear maximum: Samples SBR 0.4 and SBR 0.8 exhibit a "marching modulus". This can be explained by the lower amount of double bonds in the polymer backbone of the SBR: Their chances of crosslinking are reduced in comparison to NR. Due to that fact, t95 of SBR 1.2 (=30.0 min) is applied for these samples to limit vulcanization time. This simplification has no influence on the results.

Fig. 3 displays only one curve for every sample, which was originally tested three times: The curve with the medium value for Smax – Smin (maximum – minimum torque). The SBR-samples from Fig. 4 however could only been tested once and are thus displayed in this diagram without reference measurements. Investigated for a measurement time of 90 min, samples SBR 0.4 and SBR 0.8 did not show a torque maximum to calculate t95. All other samples went into reversion and were thus stopped manually after showing this effect.

t95 of all samples are listed in Table 4. Again, a clear tendency can be seen: The increasing content of curatives significantly reduces t95. The CBS accelerates the vulcanization process resulting in lower t95. An exception is sample NR 2.0, whose comparatively long t95 can be explained by the plateau shown in Fig. 2 and the relatively weak reversion behavior.

3.2. Qualitative analysis μ-XRF

Fig. 5 and Fig. 6 both show the results of the qualitative analysis by μ-XRF. Both reference series – NR and SBR – depict the same behavior: There are six specimens in different shades of yellow. The yellow coloration indicates at which position sulfur was detected.

The sample with the least yellow coloration can be found in the upper left corner of both figures. This can be assigned to the respective sample with the lowest proportion of crosslinking chemicals (= NR 0.4 and SBR 0.4). With increasing sulfur content, the intensity of the yellow coloration rises. It is thus already visually apparent that they differ quantitatively. However, in order to determine the real concentrations, the results still have to be quantified. This is described in the following chapter.

Due to the sample arrangement, measurement artifacts may occur at the edges of the individual cut-out samples. A more intense yellow coloration is then often displayed at these points. However, this should not be interpreted as a real increase in sulfur concentration at the edges.
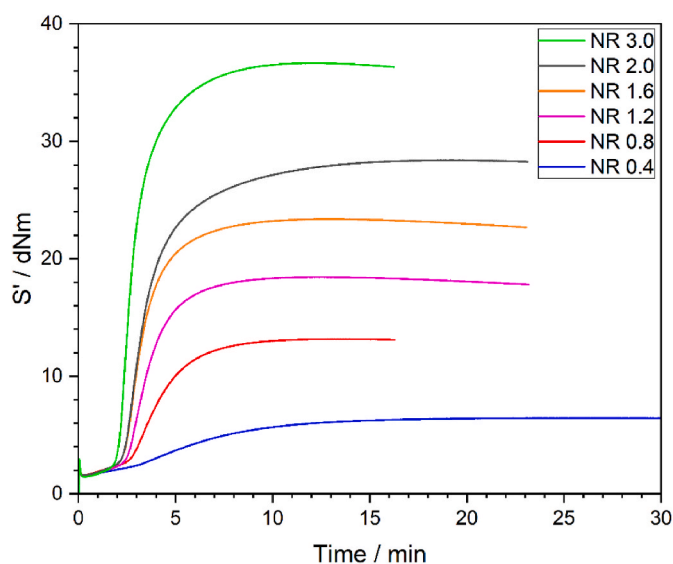

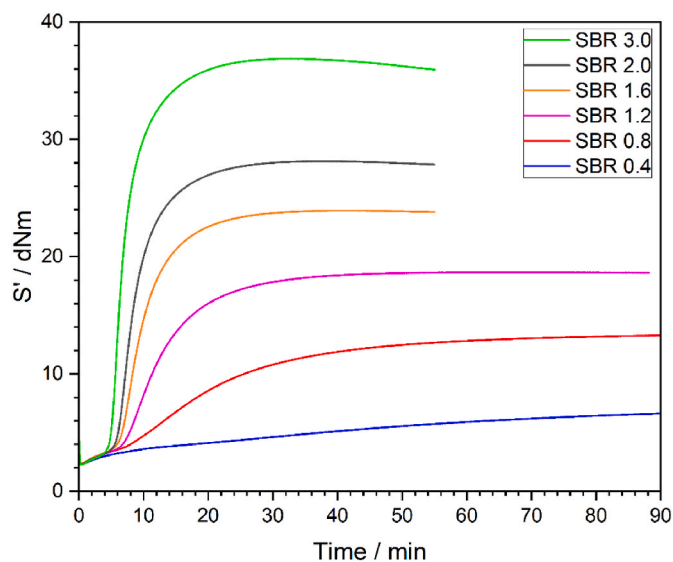**Fig. 3.** Rheometer curves of NR reference samples.

Fig. 4. Rheometer curves of SBR reference samples.

Table 4
Vulcanization times (t95) of all samples.

Sample	t95 in min
NR 0.4	14.8
NR 0.8	8.3
NR 1.2	7.1
NR 1.6	6.8
NR 2.0	9.1
NR 3.0	6.9
SBR 0.4	30.0
SBR 0.8	30.0
SBR 1.2	30.0
SBR 1.6	21.5
SBR 2.0	19.5
SBR 3.0	17.0

Besides sulfur, further chemical elements were detected during the measurements. They are listed in alphabetical order, see Table 5. Possible sources for these elements can be impurities of the natural rubber as well as other compound components. Also catalyst residues from the production of synthetic rubber are conceivable. Moreover, contaminations of the mixing equipment should be taken into account. The elements determined are taken into account in the following quantification.

3.3. Quantitative analysis μ-XRF

As described before, the fundamental parameter method has to be extended by the correction element of the chemical sum formula of the respective rubber compound. The way to determine this formula is explained in the following, using the material SBR 1.2 as an example:

First, the weight percentages $w\%_i$ of the individual compound ingredients are calculated. This is done by dividing the respective individual proportion phr_i by the total quantity phr_{Total}, see equation (1). Column 3 of Table 3 shows the results of the weight percentages.

$$w\%_i = \frac{phr_i}{phr_{Total}} * 100\% \tag{1}$$

The compound density $\rho_{compound}$ is an essential factor to calculate the total mass m_{Total} of the compound. It can be calculated using equation (2). ρ_i is the density of each individual component.

$$\rho_{compound} = \frac{phr_{Total}}{\sum \frac{phr_i}{\rho_i}} \tag{2}$$

The total mass m_{Total} of the compound is then determined by the product of $\rho_{compound}$ and the effective volume V_{eff} (in the current example 70%) (equation (3)). For sample SBR 1.2, m_{Total} is 1252.2 g.

$$m_{Total} = \rho_{compound} * V_{eff} \tag{3}$$

Equation (4) calculates the individual mass m_i of every component, the results are displayed in column 4 of Table 3.

$$m_i = \frac{w\%_i}{100} * m_{total} \tag{4}$$

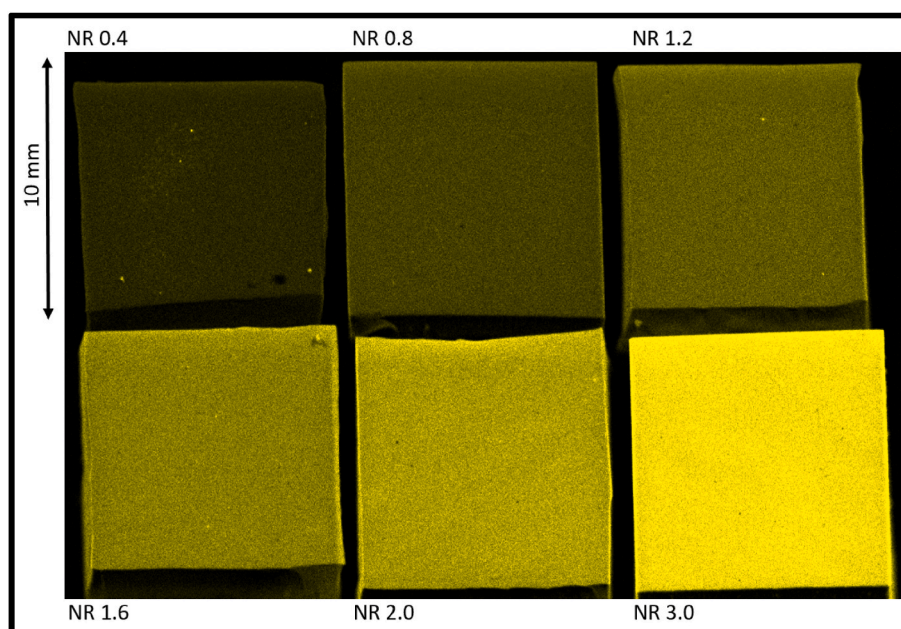The respective molecular formulas of every component can be found

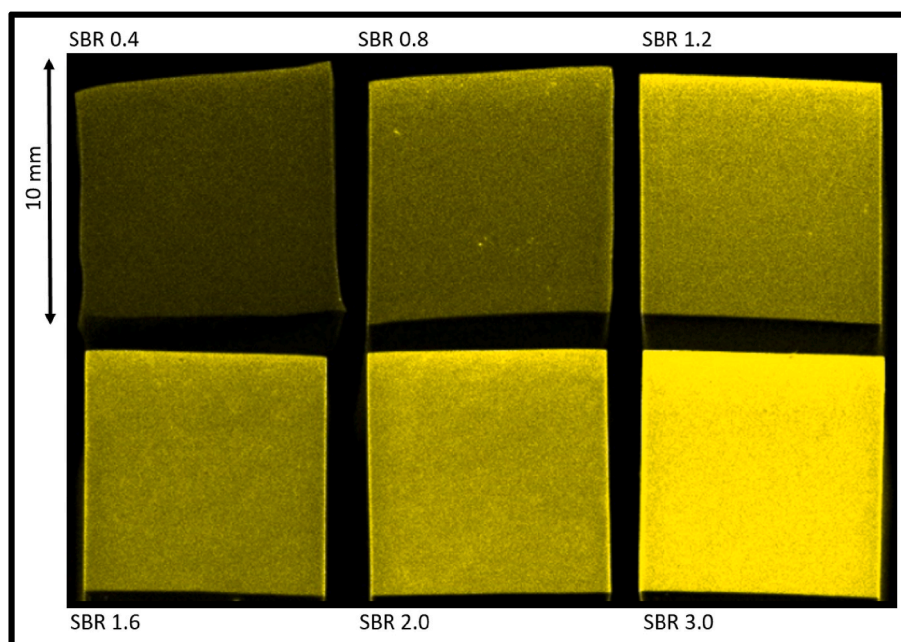**Fig. 5.** Qualitative analysis of NR reference series.

Fig. 6. Qualitative analysis of SBR reference series.

Table 5
Other detected elements of the reference samples.

NR-series	Al	Ca	Cr	Fe	K	Mn	Ni	P	–	Si	Ti	Zn
SBR-series	Al	Ca	–	Fe	K	Mn	Ni	–	Pd	Si	–	Zn

in the fifth column of Table 3. It is important to note that the empirical formula of the SBR is largely determined by the content of the styrene component (23.5%) [33]. The molecular masses M_i of the compound components are formed by the product of the relative atomic mass M_{rel} of the elements and the number n_{rel} of every element in the respective molecular formula, see equation (5). An example of the determination of M of the used stearic acid is given in equation (6). All results are listed in column six of Table 3. The values for M_{rel} are taken from Ref. [34].

$$M_i = \sum (M_{rel} \bullet n_{rel})_i \tag{5}$$

$$M_{St.\ Acid} = (M_{rel} \bullet n_{rel})_C + (M_{rel} \bullet n_{rel})_H + (M_{rel} \bullet n_{rel})_O = 12.0107\ g/_{mol}$$
$$\bullet\ 18 + 1.00794\ g/_{mol} \bullet 36 + 15.9994\ g/_{mol} \bullet 2 = 284.5\ g/_{mol} \tag{6}$$

The amount of substance n describes the amount of atoms in mol present in each component of the compound. n is determined by the ratio of m_i to M_i (equation (7)). The results for n are listed in column 7 of Table 3. In addition to that, the percentages of each component's amount of substance is shown in the last column of Table 3. This overview illustrates that sample SBR 1.2 consists of 98% of the elements carbon and hydrogen, which cannot be measured via μ-XRF.

$$n_i = \frac{m_i}{M_i} \tag{7}$$

As a next step, the above calculated n_i of each component has to be broken down into the individual proportions of every chemical element. For this, the respective proportions (see column 5 of Table 3) are calculated and multiplied by the total amount of substance n_i. This calculation is given for the example of SBR 1.2 (equation (8)):

$$n_C = \frac{4.9}{4.9 + 6.5} * 26.3\ \% = 11.3\ \%$$
$$n_H = \frac{6.5}{4.9 + 6.5} * 26.3\ \% = 15.0\ \% \tag{8}$$

An overview of the elemental distributions of all compound constituents is given in Table 6. It shows how n_i (column 2) for every component is broken down into individual proportions of every chemical element from their respective molecular formulas, which can be found in Table 3. Table 6 again emphasizes in particular the importance of the elements C and H (columns 3 and 4) for the analysis. The last row of Table 6 shows the sum of every element. The total ratio of C to H is rounded 83:15. In summary, sample SBR 1.2 consists of 99% non-detectable matter (C, H, N, O). In contrast, detectable elements Zn and S are only present in the compound to a much smaller extent (1%).

For these remaining elements, the following assumptions apply:

- Zn: About 0.5% of the atoms in sample SBR 1.2 are zinc atoms. Because zinc can be detected with μ-XRF, no further steps are necessary to quantify this element.
- N: Nitrogen cannot be detected via μ-XRF. The concentration of nitrogen atoms is very low of approx. 0.005% and is therefore neglected to simplify the composition of the non-detectable matter.
- O: Oxygen cannot be detected via μ-XRF. The majority of the oxygen is derived from the zinc oxide. The small fraction from the stearic acid is neglected for the same reason as explained for N. Via another

Table 6
Proportions of chemical elements in the total compound SBR 1.2

	n_i [%]	n C [%]	n H [%]	n Zn [%]	n N [%]	n O [%]	n S [%]
SBR	26.3	11.319	15.015				
Carbon Black	71.7	71.703					
ZnO	1.1			0.529		0.529	
St. Acid	0.2	0.058	0.117			0.006	
Sulfur	0.6						0.645
Accelerator	0.1	0.031	0.038		0.005		0.005
	100	83.111	15.170	0.529	0.005	0.535	0.649

correction factor, the oxygen is therefore coupled to the zinc with the ratio of 1:1: each time a Zn atom is detected, an O atom is deposited in the quantification calculation.

- S: About 0.6% of the atoms in sample SBR 1.2 are sulfur atoms. Because this element can be detected with μ-XRF, no further quantification steps are necessary.

In summary, two main correction elements were thus determined: First, the carbon to hydrogen ratio (83:15) calculated to 100%. Secondly, that the proportion of oxygen was formally coupled to the amount of zinc with 1:1. Supported by these correction elements, the quantification can now be carried out computer-aided with the help of the generally applicable fundamental parameters. An area of 3 × 3 measuring points is combined into one in order to reduce the computing time. This does not deteriorate the accuracy of the measurement. However, the spatial resolution is reduced.

Table 7 shows the results of the sulfur quantification of all samples by μ-XRF. First, column 2 lists the ratio of carbon to hydrogen as correction elements – termed method - used to calculate the respective samples. The number of C atoms decreases with the increase of crosslinking chemicals, while the number of H atoms remains constant. This can be explained by the fact that the molecular formula of the accelerator has more hydrogen atoms than carbon atoms. Column 3 shows the sulfur content (consisting of crosslinker and accelerator) according to the formulation in weight percent wt%. Column 4 lists the sulfur contents in wt% determined by μ-XRF using the correction elements added fundamental parameter method.

Comparing columns 3 and 4, it becomes clear that X-ray fluorescence analysis can determine the sulfur contents very accurately. The results are identical for sample NR 1.2. For samples NR 0.8, SBR 2.0 and SBR 3.0 the deviation of the sulfur content is only 0.01 w%. For other samples the difference is slightly increased. The largest difference was measured for sample NR 3.0: The concentration determined with μ-XRF is 0.09 w% below that from the formulation. One possible explanation for this could be that there was not enough curatives added to the polymer during mixing.

Fig. 7 gives an overview of the quantitative evaluation for the SBR series. It indicates that the sulfur distribution at the sample surface is very homogeneous, which can be attributed to a good distribution of curatives. The increase in sulfur concentration proceeds from SBR 0.4 to

SBR 3.0, which fits well with the results shown in Fig. 6. However, due to the aforementioned artifacts and gradient formation at the edges in Fig. 6, the identical material was measured again with μ-XRF: This time however, larger areas of 15 × 15 mm^2 were examined and subsequently the excess and artifact-prone edges were trimmed in the measurement software to create the originally intended area of 10 × 10 mm^2. After that, the quantification process was applied to the specimens."

3.4. LECO

The 832 Series Sulfur/Carbon Determinator by LECO corporation is another method to determine the sulfur content in polymer samples. The results are intended as a reference to verify that the defined amount of curatives was added to the polymer during the mixing process. The determined concentrations of sulfur are displayed in column 5 of Table 7. In principle, the values determined reflect the theoretical values from the formulation, see column 3. However, it becomes clear that the results are consistently shifted to higher concentrations. This is particularly true for the SBR series. A possible explanation for this effect could be errors in the calibration of the device. The deviations vary from 0.03% (NR 1.2) to 0.16% (SBR 1.6). The deviations for this method are thus higher than those from μ-XRF.

3.5. Comparison of μ-XRF and LECO

μ-XRF and LECO are two different measurement techniques: In the first method, the surface of a rubber sample is excited by X-rays and fluorescence radiation is used to determine the chemical elements. The sulfur determinator by LECO uses IR radiation to determine the decomposition products of a rubber sample. Both methods determine concentrations that are in the range of the expected sulfur contents. However, it becomes clear that the deviations from the theoretical values with the LECO method are significantly higher than those from the μ-XRF. This becomes visible in particular in Figs. 8 and 9.

In these diagrams, the sulfur content determined by both methods is plotted against the theoretical sulfur content according to the formulation. The original straight line (dashed line) additionally shows the theoretical content. Values plotted above this line exceed the theoretical sulfur content. Measured points below this straight line indicate determined concentrations that are below the theoretical values.

In the case of NR (Fig. 8), the values of both analysis methods are almost congruent to the theoretical sulfur content. Using the linear regression, it is clear that the offset of the LECO method is 0.088, twice that of the μ-XRF (0.045). This behavior can be explained by the deviations at low sulfur concentrations. The slope is almost identical for both methods (0.93 vs 0.94). Thus, they are almost two parallel shifted straight lines. Due to the lower offset, the results from μ-XRF match better with the theoretical values in the indicated concentration range.

This behavior becomes more apparent in the case of the SBR, see Fig. 9: The offset of the μ-XRF results is very small at 0.015. At the same time, the slope of 0.99 is close to the optimum. The results from the X-ray fluorescence are thus extremely close to the theoretical values. The slope of the LECO method with 0.98 is as high as that of the μ-XRF. However, the offset of 0.108 describes that increased values for the sulfur concentration are consistently determined. Especially at low sulfur concentrations, LECO thus shows larger deviations from the theoretically expected value. The correlation coefficients R^2 are close to the optimum for all four fits, with slightly better fits for the LECO method.

Compared to this bulk analysis, μ-XRF has several advantages: It is a non-destructive analysis. Furthermore, concentrations of other elements besides sulfur can be determined. In addition, it is possible with this technique to display the sulfur homogeneity and distribution for large areas of several cm^2. Thus, concentration differences as well as inhomogeneities can be displayed, which gives further insight views into rubber samples.
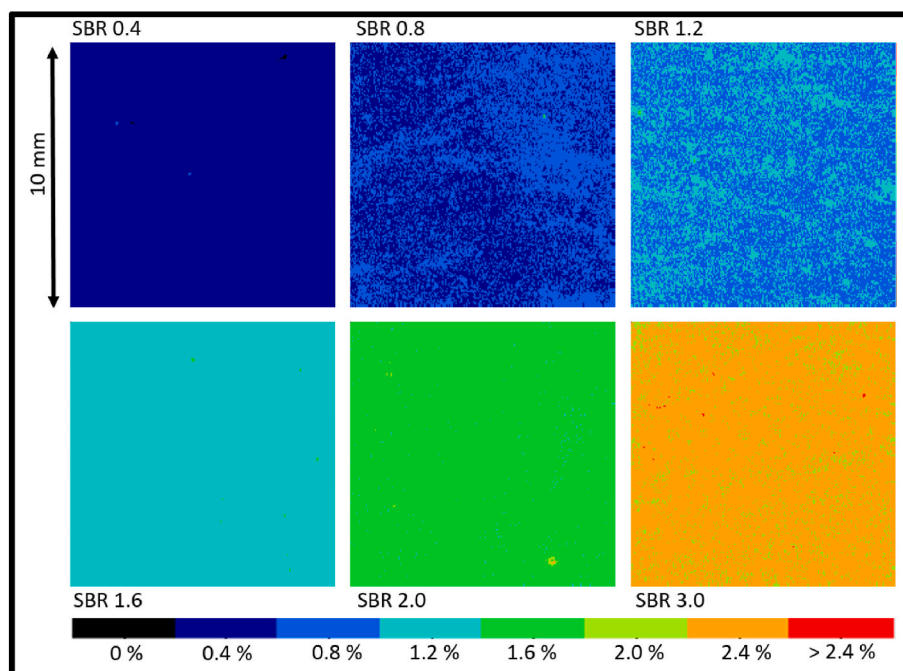
Table 7

Overview of the sulfur contents investigated by different methods.

	Method	Compound Content of S in wt%	μ-XRF calculated S in wt%	LECO S in wt%
NR 0.4	$C_{83}H_{16}$	0.31	0.34	0.38
NR 0.8	$C_{83}H_{16}$	0.62	0.61	0.68
NR 1.2	$C_{82}H_{16}$	0.93	0.93	0.96
NR 1.6	$C_{82}H_{16}$	1.23	1.17	1.24
NR 2.0	$C_{82}H_{16}$	1.53	1.51	1.55
NR 3.0	$C_{82}H_{16}$	2.27	2.16	2.23
SBR 0.4	$C_{83}H_{15}$	0.31	0.33	0.41
SBR 0.8	$C_{83}H_{15}$	0.62	0.60	0.71
SBR 1.2	$C_{83}H_{15}$	0.93	0.99	1.02
SBR 1.6	$C_{83}H_{15}$	1.23	1.17	1.33
SBR 2.0	$C_{83}H_{15}$	1.53	1.52	1.61
SBR 3.0	$C_{82}H_{15}$	2.27	2.26	2.33

Fig. 7. Quantitative evaluations of the sulfur concentrations of the SBR reference series.

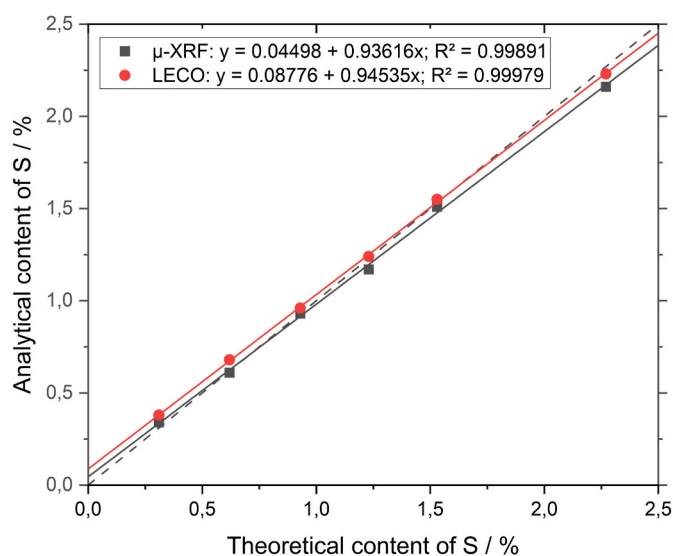**Fig. 8.** Comparison of quantitative results of both methods for NR reference series.

Fig. 9. Comparison of quantitative results of both methods for SBR reference series.

4. Summary and outlook

The μ-XRF is a tool to image the distribution of chemical elements. The quantification of these pictures is initially difficult for polymers because their main components C and H cannot be detected with this method. In this work, a way to solve this problem was shown. For this purpose, the amounts of substances of the not detectable elements were determined and used as correction parameters for the quantification with the fundamental parameter method. With this supplemented fundamental parameter method, the sulfur content can be quantified very accurately: the results fit very well with the expected theoretical values. In addition, the sulfur concentrations were confirmed by the independent method 832 Series Sulfur/Carbon Determinator by LECO Corporation.
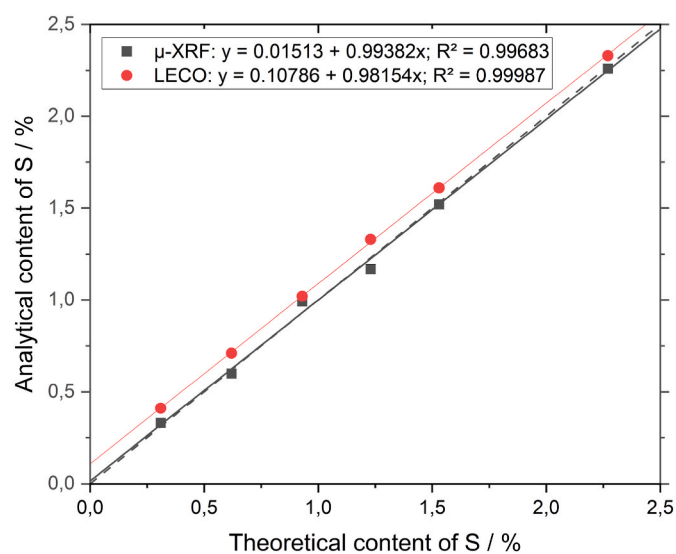
With the problem of quantification now solved, μ-XRF has a wide range of potential applications in the rubber field: The evaluation of sulfur homogeneity on elastomer surfaces of several cm^2 can now be displayed in a statistically reliable manner. This allows conclusions to be drawn about compounding quality. Other conceivable applications include investigations of the blooming or diffusion behavior of sulfur or other chemical elements. This is particularly interesting when different compounds accumulate in a product like in tires or recycled material.

Author statement

S. Frosch: Writing - Original Draft, Writing - Review & Editing, Visualization, Data Curation, Investigation, Formal analysis, Validation, Conceptualization, Methodology.

V. Herrmann: Supervision, Funding acquisition, Project

References

[1] E.W.E. van Bevervoorde-Meilof, D. van Haeringen-Trifonova, G.J. Vancso, L.v. d. Does, A. Bantjes, J.W.M. Noordermeer, Cross-link Clusters: reality or fiction? Kaut. Gummi Kunstst. 53 (7–8) (2000) 426–432.

[2] Y. Nakanishi, K. Mita, K. Yamamoto, K. Ichino, M. Takenaka, Effects of mixing process on spatial distribution and coexistence of sulfur and zinc in vulcanized EPDM rubber, Polymer 218 (Mar. 2021), 123486, https://doi.org/10.1016/j.polymer.2021.123486.

[3] H. Dohi, S. Horiuchi, Heterogeneity of a vulcanized rubber by the formation of ZnS clusters, Polymer 48 (9) (Apr. 2007) 2526–2530, https://doi.org/10.1016/j.polymer.2007.03.004.

[4] F.A. Stevie, C.L. Donley, Introduction to x-ray photoelectron spectroscopy, J. Vac. Sci. Technol. A 38 (6) (Dec. 2020), 063204, https://doi.org/10.1116/6.0000412.

[5] F. Grunert, Analytical method development to predict the in-rubber dispersibility of silica [Online]. Available: https://research.utwente.nl/en/publications/analytical-method-development-to-predict-the-in-rubber-dispersibi, 2018. (Accessed 11 September 2023).

[6] S.G. Butuc, Novel Cyclic Polysulfide Based Blends: Elucidation of the Role of Zinc Oxide in Sulfur Crosslinking, University of Twente, Enschede, 2021, https://doi.org/10.3990/1.9789036553155 [Online]. Available:.

[7] S. Frosch, V. Herrmann, F. Grunert, A. Blume, Die mikro-röntgenfluoreszenz als analysemethode in der Elastomertechnik, presented at the DKG West Conference 10 (2020). Nov.

[8] V. Herrmann, S. Frosch, T. Maslowski, D. Werner, Einsatz von definiertem Gummimehl aus NR und SBR in unterschiedlichen Matrixwerkstoffen, Gummi, Fasern, Kunstst. 74 (5) (Jan. 2021) 200–207.

[9] V. Herrmann, S. Hanning, M. Kreyenschmidt, Untersuchungen zur Diffusion des Schwefels in Rezyklat-Kautschukmischungen: teil 1: bestimmung des Diffusionskoeffizienten, Gummi, Fasern, Kunstst. 71 (5) (Jan. 2018) 232–241.

[10] V. Herrmann, S. Hanning, M. Kreyenschmidt, A. Wolff, D. Ludwig, J. Ludwig, Untersuchungen zur Diffusion des Schwefels in Rezyklat-Kautschukmischungen: teil 2: schwefeldiffusion in Mischungen mit Gummimehl, Gummi, Fasern, Kunstst. 71 (6) (Jan. 2018) 340–349.

[11] V. Herrmann, Y. Speyer, J. Leiber, Herstellung und Verarbeitung von sortenreinem Gummimehl im Labormaßstab, Gummi, Fasern, Kunstst. 70 (4) (Jan. 2017) 240–247.

[12] S.-C. Han, M.-H. Han, Fracture behavior of NR and SBR vulcanizates filled with ground rubber having uniform particle size, J. Appl. Polym. Sci. 85 (12) (2002) 2491–2500, https://doi.org/10.1002/app.10575.

[13] H. Liang, D. Rodrigue, J. Brisson, Characterization of recycled styrene butadiene rubber ground tire rubber: combining X-ray fluorescence, differential scanning calorimetry, and dynamical thermal analysis for quality control, J. Appl. Polym. Sci. 132 (42) (2015), https://doi.org/10.1002/app.42692.

[14] J. Mellawati, M. Sumarti, Y. Menry, S. Surtipanti, P. Kump, Application of X-ray fluorescence spectrometry in multielement analysis of rubber samples, Appl. Radiat. Isot. 54 (6) (Jun. 2001) 881–885, https://doi.org/10.1016/S0969-8043(00)00320-1.

[15] I. Schaumann, et al., Preparation and characterization of polymer layer systems for validation of 3D Micro X-ray fluorescence spectroscopy, Spectrochim. Acta Part B At. Spectrosc. 64 (4) (Apr. 2009) 334–340, https://doi.org/10.1016/j.sab.2009.03.004.

[16] J. Pilz, A. Maria Coclite, M.D. Losego, Vapor phase infiltration of zinc oxide into thin films of cis -polyisoprene rubber, Mater. Adv. 1 (6) (2020) 1695–1704, https://doi.org/10.1039/D0MA00304B.

[17] L. Rácz, et al., Measurement of rarely investigated trace elements as, P, Sr, Zr, Rb and Y in waste tires, Period. Polytech. - Chem. Eng. 60 (2) (2016), https://doi.org/10.3311/PPch.8101. Art. no. 2.

[18] M. Haschke, J. Flock, Röntgenfluoreszenzanalyse in der Laborpraxis, first ed., Wiley-VCH, Weinheim, 2017 https://doi.org/10.1002/9783527808816.

[19] N. Miskolczi, R. Nagy, L. Bartha, P. Halmos, B. Fazekas, Application of energy dispersive X-ray fluorescence spectrometry as multielemental analysis to determine the elemental composition of crumb rubber samples, Microchem. J. 88 (1) (Feb. 2008) 14–20, https://doi.org/10.1016/j.microc.2007.08.007.

[20] LECO Corporation, "832 Series Sulfur/Carbon Determinator: Specification Sheet, Jan. 2015.

[21] A. Pasitschniak, Determination of sulfur content by x-ray fluorescence in samples containing a single sulfide phase, X Ray Spectrum. 15 (3) (1986) 197–199, https://doi.org/10.1002/xrs.1300150309.

[22] V. Herrmann, A. Wekerle, Modification of ground rubber modification of ground rubber with conventional fillers by process engineering, Kaut. Gummi Kunstst. 8 (Jan. 2019).

[23] R. Hammer, Untersuchungen zur Vernetzungsdichte von Elastomeren mit und ohne Gummimehl: Bachelor-Thesis at University of Applied Sciences Wuerzburg-Schweinfurt, 2019. Würzburg.

[24] W.C. Röntgen, Über eine neue Art von Strahlen: 1. Mitteilung (1895), in: Über eine neue Art von Strahlen: Sitzungsberichte der physikalisch-medizinischen Gesellschaft zu Würzburg, Jahrgang 1895, S. 132 und Jahrgang 1896, S. 10, Physikalisch-medizinische Gesellschaft zu Würzburg, Springer, Heidelberg, 1949, pp. 2–11.

[25] K. Janssens, et al., Recent trends in quantitative aspects of microscopic X-ray fluorescence analysis, TrAC, Trends Anal. Chem. 29 (6) (Jun. 2010) 464–478, https://doi.org/10.1016/j.trac.2010.03.003.

[26] Welt der Physik, Was verrät die Röntgenfluoreszenzanalyse?, Jun. 10, https://www.weltderphysik.de/gebiet/teilchen/licht/synchrotronstrahlung/roentgenfluoreszenzanalyse/roentgenfluoreszenzanalyse/, 2011. (Accessed 18 July 2023).

[27] C.N. Zwicky, P. Lienemann, Quantitative or semi-quantitative?–laboratory-based WD-XRF versus portable ED-XRF spectrometer: results obtained from measurements on nickel-base alloys, X Ray Spectrum. 33 (4) (2004) 294–300, https://doi.org/10.1002/xrs.730.

[28] S. Uhlig, R. Möckel, A. Pleßow, Quantitative analysis of sulphides and sulphates by WD-XRF: capability and constraints, X Ray Spectrum. 45 (3) (2016) 133–137, https://doi.org/10.1002/xrs.2679.

[29] M. Haschke, Laboratory micro-x-ray fluorescence spectroscopy: instrumentation and applications, vol. vol. 55, in: Springer Series in Surface Sciences, vol. 55Springer, Cham, 2014.

[30] J. Sherman, The theoretical derivation of fluorescent X-ray intensities from mixtures, Spectrochim. Acta 7 (Jan. 1955) 283–306, https://doi.org/10.1016/0371-1951(55)80041-0.

[31] R.M. Rousseau, The quest for a fundamental algorithm in X-ray fluorescence analysis and calibration, Open Spectrosc. J. 3 (1) (Jan. 2009) 31–42, https://doi.org/10.2174/1874383800903010031.

[32] S. Flude, M. Haschke, M. Storey, Application of benchtop micro-XRF to geological materials, Mineral. Mag. 81 (4) (Aug. 2017) 923–948, https://doi.org/10.1180/minmag.2016.080.150.

[33] ARLANXEO Deutschland GmbH, BUNA se 1502 L: Product data sheet. https://www.arlanxeo.com/en/E-SBR/Buna%C2%AE/p/buna-se-1502-l#.

[34] B. Kahn, Radioanalytical Chemistry, Springer, New York, 2007.